The Journal of Experimental Biology 210, 765-780
Published by The Company of Biologists 2007
doi:10.1242/jeb.02690

Response properties of primary afferents supplying Eimer's organ

Paul D. Marasco[1] and Kenneth C. Catania[2,*]

[1]*Neuroscience Graduate Program and* [2]*Department of Biological Sciences, Vanderbilt University, Nashville, TN 37235, USA*

*Author for correspondence (e-mail: ken.catania@vanderbilt.edu)

Accepted 12 December 2006

Summary

The mole's nose is covered with mechanosensory structures called Eimer's organs. Each organ contains Merkel cell-neurite complexes, Paciniform corpuscles and intraepidermal free nerve endings. The function of Eimer's organ has been the subject of speculation since the 1800s, but responses from the afferents have never been investigated. Our goal was to explore the function of Eimer's organ by recording primary afferent responses to a range of mechanosensory stimuli. Unit activity from the trigeminal ganglion was recorded from coast (*Scapanus orarius*) and star-nosed (*Condylura cristata*) moles, while stimulating the nose with a Chubbuck mechanosensory stimulator, a piezo-electric sweeping stimulator, and hand-held probes. Stimuli included static indentations, sinusoidal displacements, different indentation velocities, displacement amplitudes, and directional stimuli across the skin. Receptive fields were small, sometimes restricted to single Eimer's organs. Responses were consistent with a slowly adapting Merkel cell-neurite complex-like receptor class and a dynamically sensitive Pacinian-like rapidly adapting class. A second rapidly adapting class was hypothesized to represent activity of prominent free nerve endings within a central cell column. Some receptors were most sensitive to stimuli applied in particular directions across the skin. Most receptors relayed mechanosensory input with high temporal fidelity. In addition some receptors were tuned to respond best when stimulated at a velocity matching the velocity of the nose during foraging. These results support the hypothesis that Eimer's organ functions to detect small surface features and textures by encoding and integrating deflection information for multiple Eimer's organs during brief touches.

Key words: mole, insectivore, touch, directional tuning, free nerve ending, receptive field, phase locking, trigeminal ganglion, skin, epidermis, sense, merkel cell.

Introduction

Moles are experts at finding prey and navigating dark underground tunnels using the tip of their snout to make sensory discriminations. A close examination of the nasal skin of talpid moles reveals a dense array of small (60 μm) raised bumps. These bumps are specializations of the epidermis called Eimer's organs (see Eimer, 1871). Each organ contains Merkel cell-neurite complexes (MCs) lamellated corpuscles (LCs) and a collection of geometrically arranged free nerve endings (FNEs) within a central cell column (Fig. 1). Arrays of Eimer's organs are the most densely innervated areas of skin to be found in mammals (Catania and Kaas, 1997) and the predictable arrangement of associated sensory receptors has made them a convenient model system for examining nerve endings. Pioneers of nervous system anatomy, such as Ranvier (Ranvier, 1880; Ranvier, 1889) Merkel (Merkel, 1875; Merkel, 1880) and others (Retzius, 1892; Bielschowsky, 1907; Dogiel, 1903; Botezat, 1903; Kadanoff, 1928; Boeke, 1932; Boeke, 1940; Boeke and deGroot, 1907; Groeneweg, 1923) made frequent use of Eimer's organ to examine mammalian sensory receptors.

Eimer's organ has also been of interest more recent (Cauna and Alberti, 1961; Quilliam, 1966a; Quilliam, 1966b; Andres and von Düring, 1973; Gorman and Stone, 1990; Catania, 1995a; Catania, 1996; Marasco et al., 2006) because the conspicuous and stereotypic structure of associated nerve endings suggests they are performing unique functions that underlie the ability of moles to make rapid sensory discriminations (e.g. Catania and Remple, 2004; Catania and Remple, 2005). It has been suggested from anatomical studies that Eimer's organ could function to detect minute surface textures through the differential deflection of the central cell column and subsequent selective activation of parts of the circular arrangement of associated nerve terminals (Catania, 2000). The circular arrangement of nerve terminals is found in Eimer's organ of nearly every mole species (Catania, 2000) and a similar structure, the push rod, is found in monotremes (Andres and von Düring, 1984; Andres et al., 1991; Manger and Hughes, 1992; Iggo et al., 1996; Manger and Pettigrew, 1996). Comparative evidence indicates that push rods and Eimer's organs are analogous structures and that monotremes

and moles independently arrived at the same structural solution for increasing tactile acuity of the skin.

Despite a longstanding interest in the structure and function of Eimer's organ, nothing is known about response properties of the primary afferent neurons that serve the organ and transmit information to the CNS. This is probably because, historically, insectivores have been difficult to anesthetize for electrophysiological investigations (e.g. Allison and Van Twyver, 1970) and the anatomy of their trigeminal system differs from that in more common laboratory animals. However, advances in the ability to anesthetize small mammals have allowed neural recordings to be made even from small-brained shrews (e.g. Catania et al., 1999) and moles (Catania and Kaas, 1995) and it is now possible to apply these techniques to investigating subcortical components of their CNS.

In this study, single unit electrophysiological recordings were made from primary afferents at the level of the trigeminal ganglion of star-nosed moles and coast moles to examine the response properties of receptors within Eimer's organ. A range of different stimuli were used to help distinguish different receptor subclasses and to examine threshold sensitivity to different amplitudes of step displacements and indentation velocities. We also used directionally applied stimuli to assess the ability of the receptors to code for differential displacements of Eimer's organ. Although some of the longer analyses were only possible from a limited number of cells, the results provide important new insights and support the hypothesis that Eimer's organ transduces textural information from objects in the environment.

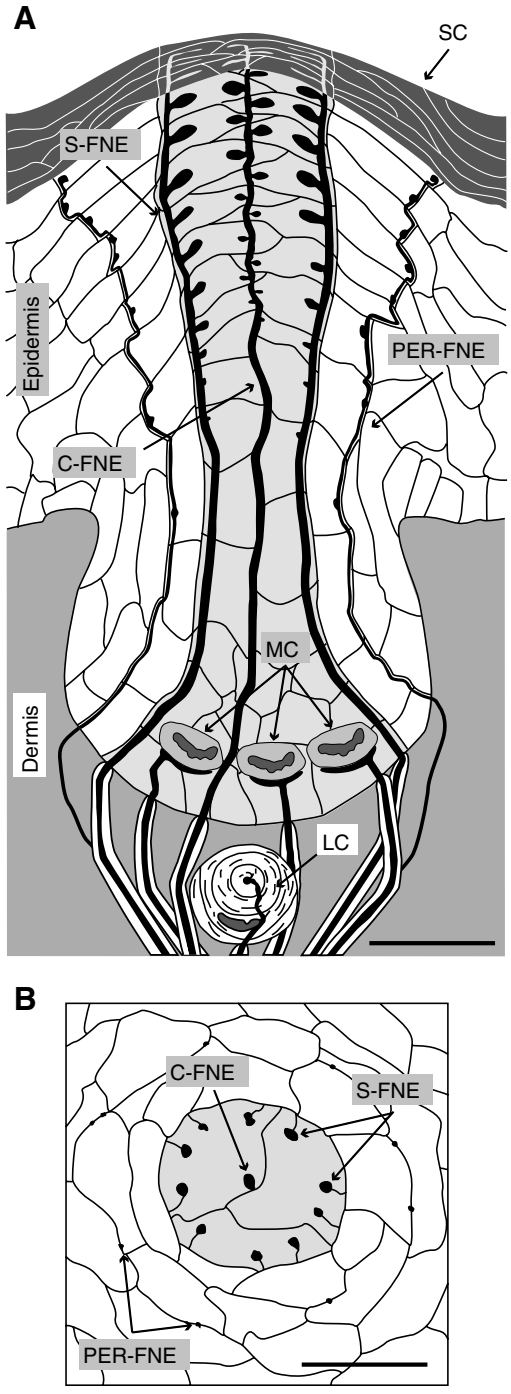

Fig. 1. The structure of Eimer's organ in the coast mole *Scapanus orarius*, viewed from the side (A) and from above (B). A central column of epithelial cells is associated with mechanoreceptive intraepidermal free nerve endings arranged in a ring (C-FNE and S-FNE). A second set of smaller nociceptive free nerve endings surrounds the central column (PER-FNE). Merkel cell–neurite complexes are arrayed at the base of the Eimer's organ (MC) and one to two lamellated corpuscles (LC) are found below the Merkel cell-neurite complexes. SC, stratum corneum. Scale bars, 20 μm. (Adapted from Marasco et al., 2006.)

Materials and methods

Two star-nosed moles *Condylura cristata* (Linnaeus 1758) were collected in Pennsylvania under permit COL00087 and eleven coast moles *Scapanus orarius* (True 1896) were provided by Dr Kevin L. Campbell of the University of Manitoba (Winnipeg, Canada). Procedures were approved by the Vanderbilt University Institutional Animal Care and Use Committee and followed NIH guidelines.

Animals were anesthetized with an intraperitoneal dose of 1.0 g kg^{-1} urethane supplemented with 20 mg kg^{-1} ketamine hydrochloride and 0.5 mg kg^{-1} xylazine as needed for a surgical plane of anesthesia. A craniotomy was performed over the left trigeminal ganglion and frontal cortex was aspirated to expose the ganglion on the floor of the skull. Extracellular responses were recorded from trigeminal ganglion with large-diameter (250 μm), 12° taper, epoxy insulated tungsten microelectrodes (5 MΩ at 1 kHz; A-M Systems Inc., Carlsborg, WA, USA). Data were collected using a Cambridge Electronic Designs (CED) Power 1401 computer interface and Spike 2 software. After recordings, animals were killed with 150 mg kg^{-1} sodium pentobarbital and perfused with 1× phosphate-buffered saline (PBS) pH 7.3 followed by 4% paraformaldehyde (PFA) in PBS.

Using a surgical stereomicroscope, the receptive field (RF) for each response was determined by hand with a blunted insect pin and drawn on a schematic of the snout. A Chubbuck mechanosensory stimulator (Chubbuck, 1966) and a piezo bending element stimulator (Piezo Systems Inc., Cambridge, MA, USA) were then applied for compressive and sweeping stimuli, respectively. Stimulators were mounted on micromanipulators and were controlled by the CED unit. Compressive stimuli from the Chubbuck stimulator were applied through an acrylic tip tapered to 0.5 mm. For three single units, a blunted insect pin was attached to the Chubbuck in order to stimulate individual Eimer's organs. The position of the Chubbuck probe tip was monitored by recording the pickoff circuit output signal in Spike 2. During data collection the probe tips, at resting position, were brought into contact with the surface of the nose using a stereomicroscope.

Responses to indentation stimuli were measured by subjecting the RF for each cell to five banks of 100 sinusoidal cycles at frequencies of 10, 50, 100, 150, 200, 250 and 300 Hz. Each five-bank frequency run was repeated at displacement amplitudes of 1, 5, 10, 20 and 28 μm. Responses that followed with 98–102 spikes for each set of 100 cycles were considered 1:1 (Gibson and Welker, 1983). Fewer responses were considered intermittent. If no responses were elicited the RF was subjected to larger displacements (0–600 μm at 5 Hz, 0–600 μm at 10 Hz, 0–580 μm at 25 Hz, 0–535 μm at 50 Hz, 0–235 μm at 100 Hz, 0–180 μm at 150 Hz, and 0–50 μm at 200 Hz). This paradigm allowed responses for each frequency of stimulation to be broken down into 1:1 response ranges, intermittent response ranges, and no-response ranges.

Depression thresholds were measured in response to step indentations of 1, 5, 10, 25, 50, 75, 100, 125 and 150 μm. Each indentation consisted of a square wave that lasted for 500 ms with an 84.5 mm s^{-1} onset and retraction velocity. Five individual banks of 10 indentations were applied at each displacement increment. Responses were considered 1:1 if all 50 indentations elicited a response; fewer responses were considered intermittent.

Velocity-dependent responses were measured with ramp indentations applied with onset velocities of 3.0, 10.0, 25.0, 46.2 and 84.5 mm s^{-1}. Each ramp had a 500 μm displacement and five individual banks of 10 indentations were applied at each onset velocity. Responses were considered 1:1 if all 50 indentations elicited a response; fewer responses were considered intermittent. As part of this analysis a velocity of 46.2 mm s^{-1} was chosen because it matched the velocity of the nose during touches in behaving moles (from high-speed video analysis).

Directional sensitivity was tested with a sweeping 2 mm diameter wooden probe, with a 1 mm rounded tip, fixed to a piezo bending element. When the directional sensitivity of a cell could be determined with a hand-held probe the sweep axis of the bending element was aligned with the direction of maximal sensitivity. The stimulator was swept back and forth across the center of the receptive field in five banks of 100 cycles at 2 Hz. The piezo stimulator was then rotated clockwise 60° and the 500 cycles were repeated. The stimulator was then rotated an additional 60° and 500 cycles were repeated. In two cases where there was little activity in directions other than the initial 0° sweep, the stimulator was rotated another 60° clockwise to 180° as a control to ensure that the cell was still responding. When no directionality could be established with the hand probe, the sweep axis for the stimulator was initially aligned in a random direction.

The responses for each direction were sorted into 60° bins. To facilitate comparisons, histograms were rotated so that the maximally responsive direction was aligned to 0° and the responses at other directions were normalized as a percentage of the maximum. After normalization, three different methods of analysis were used to evaluate directional sensitivity of each receptor. The Rayleigh test was used as a liberal measure of directionality (Batschelet, 1981; Fisher, 1993; Zar, 1999). The Rayleigh Z value (Rz) and P values were calculated using Oriana (Kovach Computing Services, Isle of Anglesey, Wales, UK) and were considered significant at $P<0.05$. Next, the tuning ratio (*TR*) and tuning index (*TI*) were used as measures of directional sensitivity (Minnery and Simons, 2003). The *TR* is the ratio of the average response across all directions to the maximal response. The *TR* was established for each unit by taking the proportion of responses for each direction compared to the number of responses elicited at the maximally active direction (taken as 100%). The resulting proportions were averaged and divided by 100 to yield the *TR*. The *TI* was calculated by determining the number of directions with response proportions that were significantly smaller than the response proportion at the maximum direction. Comparisons between the mean values of the response magnitudes were made at the $P<0.05$ level using the Student–Newman–Kreuls method for pair-wise multiple comparisons. Calculations were performed using SigmaStat (Systat Software, Inc., Point Richmond, CA, USA).

To determine the degree of phase locking, cycle histograms (CH) were generated from the responses to sinusoidal mechanical stimulation. One hundred impulses, collected at the frequency of peak activation, were used to construct the CH for each cell so that comparisons could be made across all recordings. The location in degrees of each response was calculated with respect to a set starting point for each cycle and bin widths for each histogram were calculated to represent a window of 0.1 ms so that the temporal resolution for each histogram would be equal regardless of frequency. The length of the mean vector [*resultant* (*R*)] was calculated for each distribution (see Lavine, 1971; Bledsoe, Jr et al., 1982; Vickery et al., 1992; Coleman et al., 2001; Mahns et al., 2003). For a CH with a sample size of 100 or more impulses, an R value <0.17 indicates no phase locking. Conversely, R values >0.3 are indicative of a very high degree of phase locking (Durand and Greenwood, 1958; Bledsoe, Jr et al., 1982; Coleman et al., 2001; Mahns et al., 2003).

Results

Recordings were made from a total of 55 primary afferent mechanosensory neurons serving the glabrous rhinarium of the coast mole. The recording sessions were conducted in two phases, a qualitative mapping phase and a quantitative examination phase.

In the first phase, the activity from 33 neurons was examined. The general mapping experiments in these three animals were undertaken to explore the layout of the trigeminal ganglion. The rostral/medial portion of the ganglion provided the most afferents with RFs on the rhinarium [consistent with previous investigations (see Gregg and Dixon, 1973)]. The RF and general response properties were qualitatively documented for each receptor (Fig. 2). The receptors were placed into two broad classes depending on their response to sustained compression of the skin. If the surface of the nose was depressed for a prolonged period with a hand probe and the cell responded only to the onset of the stimulus we considered that neuron to be rapidly adapting (RA). If a neuron responded continuously to the indentation the receptor was classified as slowly adapting (SA). In addition a number of the cells showed an obvious preference to having the probe brushed across the RF in a particular direction. When this type of response was encountered the cell was considered to be directionally sensitive (DS). Of the 33 cells examined in the qualitative phase, 26 (78.8%) were RA and 7 (21.2%) were SA. Within the population of RA responses 6 (18% of all of the neurons, 23.1% of the RAs only) responded in a directionally selective manner to stimuli that were applied with the hand-held probe in a brushing motion parallel to the surface of the skin.

In the second phase of the experiments the response properties from 22 cells in eight animals were quantitatively analyzed with respect to sinusoidal (mechanical frequency) tuning properties, skin indentation thresholds, static displacements, stimulus onset velocity, and directional sensitivity. These neurons were broadly classified as RA or SA by response to a 500 μm static indentation lasting for 500 ms. Within the scope of the quantitative phase 21 (95.5%) of the cells were classified as RA because they responded only to the dynamic portions of the stimulus. One cell (4.5%) responded to both the dynamic and static portion of the stimulus and was classified as SA.

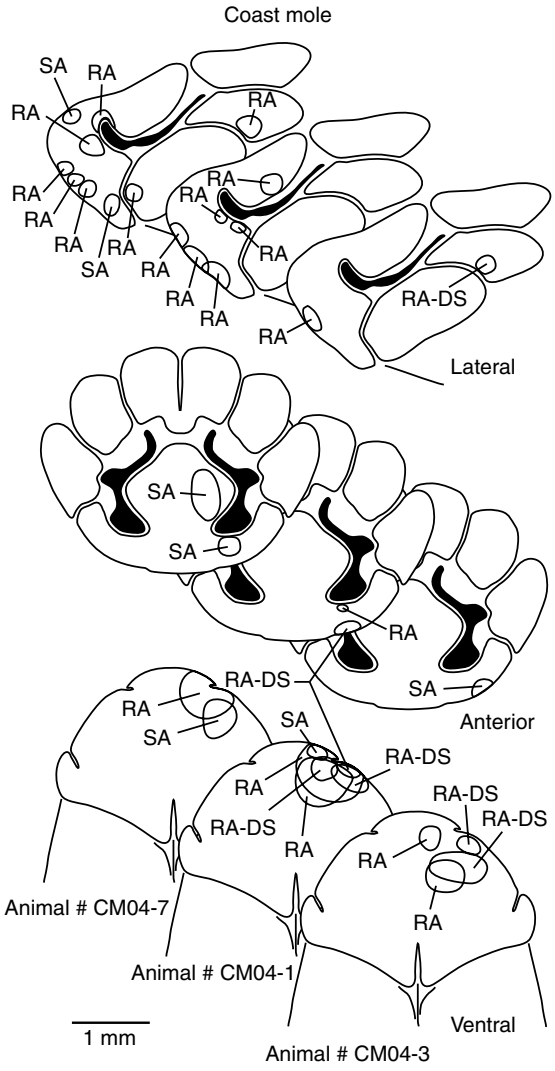

Fig. 2. Single unit receptive field diagrams for three coast moles (left to right). SA, slowly adapting neurons; RA, rapidly adapting neurons; DS, directionally sensitive receptors.

Receptor classes

Three distinct sub-types of responses were evident across the broad RA and SA classifications. The SA response showed a typically Merkel cell-like response to a static displacement (Fig. 3A). This was seen as the characteristic robust response to the initial dynamic phase of the compression followed by an irregular discharge during the sustained portion of the indentation (Iggo and Muir, 1969). Within the RA category two patterns of discharge relating to static indentation were evident. The first was a Pacinian corpuscle-like response profile, showing a response to changes in the dynamic portions of the indentation with no response during the static phase (Loewenstein, 1958; Talbot et al., 1968). The second group of response profiles showed a single impulse at the onset of the stimulus and no activity during the static phase. Receptors exhibiting this response profile occasionally fired one impulse upon retraction of the stimulator for compressions longer than 500 ms.

Recording experiments using the star-nosed mole appeared to show a similar division of receptor response profiles. Fig. 4 shows the traces for six single units, which correspond well to the responses seen in the coast mole. Three receptors (Fig. 4D–F) showed typical Merkel-like response to static compression and two cells (Fig. 4C,G) showed Pacinian-like (PC-like) responses; however, neither cell fired at the retraction of the stimulus. One RA cell (Fig. 4B) responded with a single impulse at the onset of the compression and also responded in a directionally selective manner.

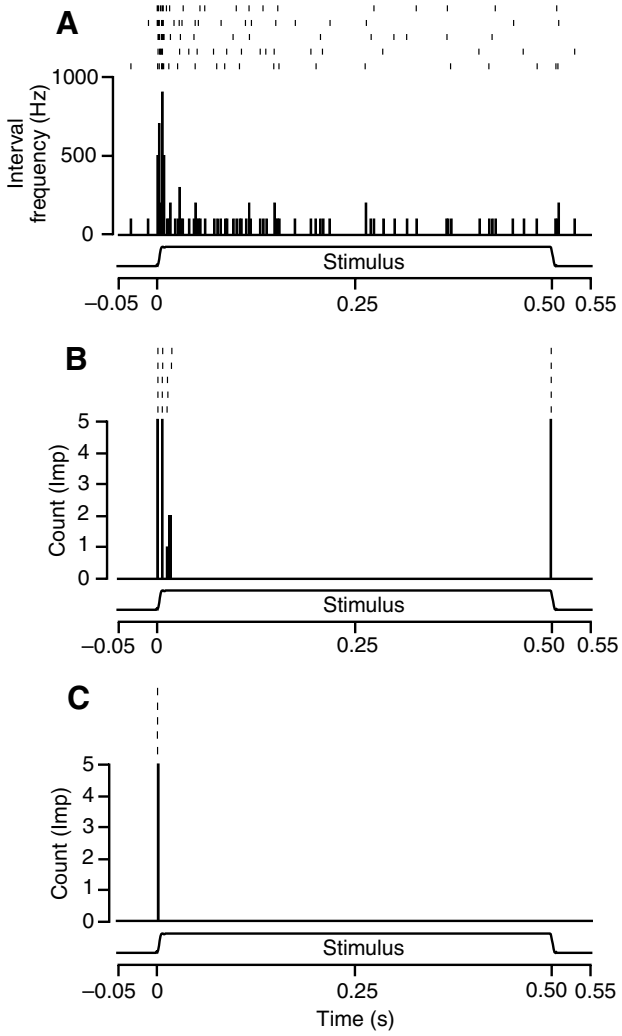

Fig. 3. Peristimulus time histograms showing three receptor response profiles found during the quantitative phase of experiments in the coast mole. (A) Slowly adapting Merkel-like response with a high dynamic sensitivity and a random sustained discharge. (B) Rapidly adapting Pacinian-like (PC-like) response sensitive to changes in the dynamic phase of the indentation with no response to the static portion of the indentation. (C) Rapidly adapting response to the compressive phase of the indentation and silent through the static phase. This response is hypothesized to be from the intraepidermal free nerve endings. Imp, impulses.

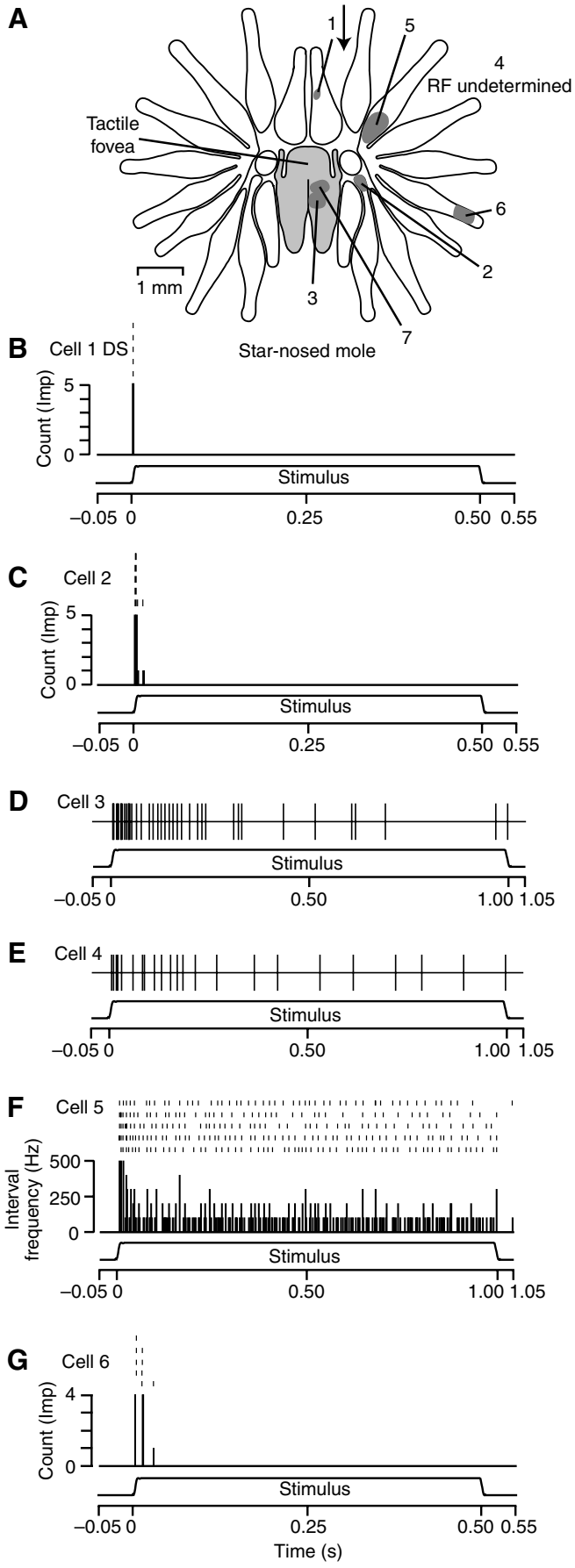

Fig. 4. Peristimulus time histograms and electrophysiological traces showing responses from the star-nosed mole. (A) The receptive field (RF) for each cell is presented on a schematic of the mole's nose. (B–G) Three classes of receptor were evident, showing the following responses: (D–F) Merkel-like response; (C,G) Pacinian-like response; (B) an RA response to the onset of compression. This receptor was also directional. An arrow on the RF diagram shows the preferred direction. Imp, impulses.

Peak activation frequency

An interesting pattern in the RA response to compressive stimuli emerged during the recording sessions. There seemed to be RA receptors that were relatively unresponsive to compressive stimuli of any type but were acutely responsive to any kind of stimulus that brushed or slid across the surface of the nose. These receptors were generally activated by compressive stimuli applied with large displacements and high velocity. By contrast there were a great number of RA receptors that responded robustly to small magnitude compressions of any kind but that were not as clearly responsive to the sweeping stimuli.

When sinusoidal compressive stimuli were applied to the RA receptors a quantitative distinction between these two qualitative measures also became evident. The receptors that were very sensitive to sweeping stimuli and difficult to activate with compressive stimuli were maximally activated across a broad range of frequencies, running from 5–150 Hz, at large displacements, ranging from 85–485 μm. Conversely, the receptors that were more responsive to compressive stimuli showed a narrow peak of maximal activity at 250–300 Hz with displacements that were an order of magnitude smaller, extending from 10–28 μm. Fig. 5 shows the frequency at which these cells were maximally sensitive (the smallest displacements that activated them robustly) for each cell that was held long enough to record the full course of sinusoidal mechanosensory data. There were two clusters of response properties evident, one in the upper left of the graph (high frequency and small displacements) and one at the lower right (low frequency and large displacements). On the basis of the tight clustering of RA receptors maximally tuned to frequencies of 250–300 Hz at relatively small displacements, these neurons were classified putatively as PC-like in nature. This follows from the general diagnostic features of Pacinian activity with maximal activation at 200–300 Hz (Sato, 1961; Jänig et al., 1968; Talbot et al., 1968; Johansson et al., 1982; Bolanowski, Jr and Zwislocki, 1984; Mahns et al., 2003). The receptors that were more diffusely clustered in the low frequency, large displacement range were classified putatively as rapidly adapting-unknown (RA-X) cells. Two cells maximally active at 150 Hz fell into intermediate categories. However, more detailed examination of their response profiles allowed them to be tentatively assigned to specific classes (see Fig. 5).

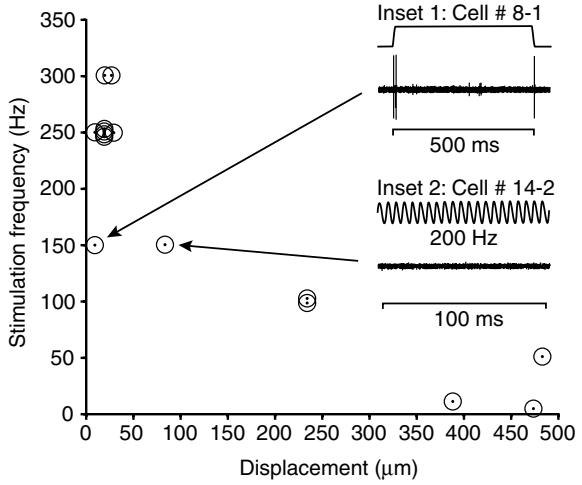

Fig. 5. Plot of the frequency of maximum sensitivity for all RA cells. Two distinct populations were evident. One cluster of units was most responsive to sinusoidal compression at 250–300 Hz with displacement of 20 and 28 μm. A more diffuse cluster of units (lower right) was most responsive to sinusoidal compression ranging from 5-100 Hz at amplitudes from 100–485 μm. The upper left group was classified as Pacinian-like (PC-like) whereas the lower right group was classified as RA-unknown (RA-X). Two receptors were intermediate. Both showed peak activation at 150 Hz but one (cell 8-1) responded to a 10 μm displacement and the other (cell 14-2) responded at an amplitude of 85 μm. Inset 1 shows the response of 8-1 to static displacement in a PC-like manner. Inset 2 shows cell 14-2 was unresponsive to sinusoidal compression at 200 Hz and so was classified as RA-X.

Quantitative receptive fields

RFs were found to be extremely small: averaging 119 μm in diameter and ranging from 70 to 210 μm, measured across the longest axis. The RFs were represented on the composite schematic (Fig. 6) according to the following classes: Merkel-like, PC-like, RA-X, and RA-incomplete classification (RA-IC). The cells labeled RA-IC were qualitatively determined to be RA but were not held long enough during recording to allow definitive characterization. There was little difference in the diameter of the RFs between the PC-like (mean = 94.4 μm), RA-X (mean = 119.2 μm) and RA-IC (mean = 128.3 μm) receptors; however, the single Merkel-like response was somewhat larger in diameter (275 μm).

Indentation velocity

When we stimulated the skin surface containing Eimer's organ with handheld probes, some receptors responded most robustly to taps. These responses seemed consistent with mole behavior, as moles repeatedly tap and probe the ground with their nose while foraging. The velocity at which the nose contacts the substrate was determined from high-speed video to be an average of 46.2 mm s^{-1}. To examine afferent responses to different velocities of indentation, a 500 μm displacement ramp stimulus was applied at 3.0, 10.0, 25.0, 46.2 and 84.5 mm s^{-1} (84.5 was the maximum velocity attainable).

The effects of indentation velocity were examined across 13 RA receptors (Fig. 7A). Our goal was to determine the lowest indentation velocities at which the receptors responded, as this is another measure of sensitivity to mechanical stimuli. We found that for a number of cells (five, or 39%) the minimal velocity at which they responded (at 1:1) was 46.2 mm s^{-1}, corresponding to the approximate speed of the nose during foraging behavior. In addition, for two cells (15%) the minimal velocity for 1:1 responding was 84.5 mm s^{-1}, for three cells it was 25 mm s^{-1} (23%), for one cell (8%) it was 10 mm s^{-1} and for two cells (15%) is was 3 mm s^{-1}. When examined by subclass, the PC-like units tended to be active at 1:1 threshold

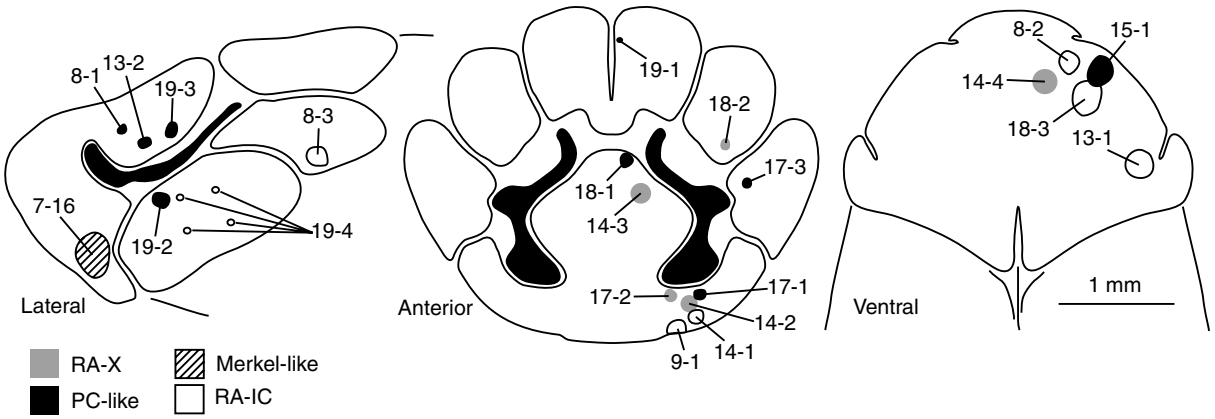

Fig. 6. Composite drawing of the coast mole nose showing all of the RFs from the quantitative phase of the experiments. Each RF is labeled with its respective cell number and receptor sub-classification. PC-like, Pacinian-like; RA-X, rapidly adapting-unknown; RA-IC, rapidly adapting-incomplete classification.

for a broad range, starting at 3 mm s^{-1} and ending at 46.2 mm s^{-1}. Conversely, the RA-X units tended to respond at 1:1 across a slightly smaller range, beginning at the higher indentation velocities (25–84.5 mm s^{-1}). The RA-IC unit responded at 1:1 through the entire range of indentation velocities.

The cells were also examined in terms of the lowest indentation velocity required to elicit any response [i.e. absolute threshold (Mahns et al., 2003)] (Fig. 7B). There was a trend toward absolute threshold activation at the lower velocities. Five units (39%) responded at absolute threshold beginning at 3 mm s^{-1}, three cells (23%) were active beginning at 10 mm s^{-1}, one (8%) at 25 mm s^{-1}, two (15%) at 46.2 mm s^{-1} and two (15%) at 84.5 mm s^{-1}. When examined according to class, the PC-like units responded at generally lower velocities of indentation (Fig. 7A). Conversely, the RA-X units tended to respond at higher indentation velocities: 67% at 46.2 mm s^{-1} and above.

Two RA cells had a velocity-dependent response to the ramp stimuli (Fig. 7C). These units generally fired multiple pulses upon indentation and both cells were active at 1:1 threshold in response to all velocities. In each case, from velocities of 3 mm s^{-1} up to 46.2 mm s^{-1}, the instantaneous average frequency of the inter-spike intervals increased as the velocity of the indentation increased. Interestingly, the average interval frequency in both units appeared to be tuned near the behaviorally relevant velocity (46.2 mm s^{-1}). Cell 19-4 plateaued in average interval frequency above 46.2 mm s^{-1} and cell 19-2 decreased in the average interval frequency above

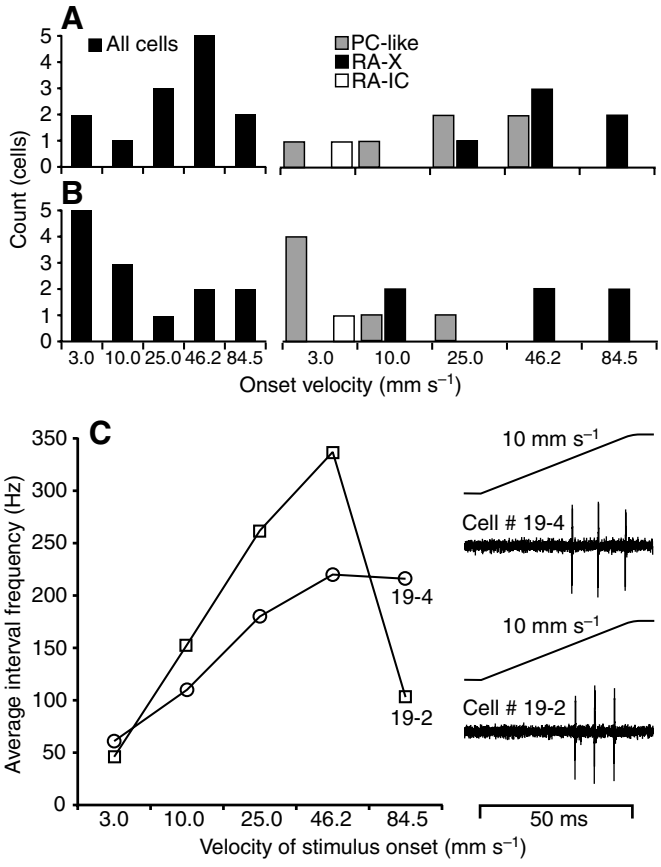

Fig. 7. Receptor responses to indentation velocity related to the speed at which the mole touches its nose to the ground (46.2 mm s^{-1}). (A) Lowest indentation velocity required to elicit a 1:1 for RA units (Left). A number of cells were most activated near the behaviorally relevant speed. The same graph is divided by sub-class on right. (B) Lowest velocity required to elicit any response. (Left) Most cells responded at less than 1:1 to the lower velocities. (Right) The same graph divided by sub-class. The PC-like units tended to be responsive at the lowest velocity and as such were more sensitive than the RA-X group. (C) Stimulus response relations for two cells that appeared to code indentation velocity (Left). As indentation velocity increased, the average interval frequency increased. Both cells appeared to be tuned near the behaviorally relevant velocity of 46.2 mm s^{-1}. (Right) Responses during the ramp indentation. PC-like, Pacinian-like; RA-X, rapidly adapting-unknown; RA-IC, rapidly adapting-incomplete classification.

46.2 mm s^{-1}. Cell 19-2 was classified as PC-like and cell 19-4 was categorized as RA-IC because we were unable to apply sinusoidal stimuli to provide subclass assignment.

Depression thresholds

The static indentation threshold levels of 13 RA receptors were evaluated by applying 50-ms duration step indentations at a range of displacements running from 1 to 150 μm (Fig. 8). Of the 13 units, five did not respond at any level to indentations ⩽150 μm. Of those that responded, none fired at 1:1 for displacements smaller than 125 μm. Three cells fired at 1:1, starting at 150 μm, and one unit did not respond at 1:1 for any displacement. Although the 1:1 responses of the PC-like and RA-X classes were similar, the two groups have different absolute thresholds. The PC-like group was most sensitive to small displacements. In particular, one PC-like unit responded to static displacements of 5 μm. The other three units in the PC-like class responded at absolute levels to displacements at 50, 75 and 125 μm. The RA-X group did not respond to displacements smaller than 125 μm.

Directional sensitivity

During qualitative mapping experiments in both the coast mole and the star-nosed mole we found receptors preferentially activated by directional stimuli (see Figs 4, 9). Fig. 9 shows the composite receptive fields for these receptors with preferred direction in the coast mole. Directional data were gathered from a total of 17 units. Fig. 10A–C shows the directional histograms and receptive fields of representative units from each subclass. All but two receptors examined were significantly directional by the Rayleigh test (Table 1). Six (35%) of the units had *TR* values less than 0.5 and four (24%) units had *TR* values less than 0.6. The average *TR* value for all the units was 0.53, ranging from 0.19 to 0.73 (Table 1). Eight units (47%) had *TI*s of 5 and one (6%) cell had a *TI* of 4. This indicates that 53% of the neurons examined were highly directionally tuned. The average *TI* for all receptors was 3.5 and ranged from 0 to 5 (Table 1).

Two receptors, cells 18-2 and 13-1, stood out as being almost entirely silent in non-preferred directions (Fig. 10C,D). Receptor 13-1 had an *Rz* of 46.98 with a *P* value of 0, a *TR* of 0.27 and a *TI* of 5. Receptor 18-2 had an *Rz* of 94.31 with a *P* value of 0, a *TR* of 0.19 and a *TI* of 5 (Table 1). Cell 18-2 was nearly completely directionally tuned by all measures. These two most profoundly directional units were part of the RA-X population. Directional tuning within the PC-like class appeared to be less distinct than in the RA-X class and the single Merkel-like receptor (see Table 1). Normalized response magnitudes for each direction were averaged for the RA-X and PC-like populations so that a graphical comparison could be made between the two. Fig. 11 shows that whereas both populations are directionally tuned the RA-X class is more narrowly tuned than the PC-like class.

Temporal patterning

All of the units analyzed showed a considerable capacity for phase locking. The average *R* value for all of the cells together was 0.953, as measured with bins equaling 0.1 ms for all peak frequencies ranging from 10 to 300 Hz. Nine receptors (69%) had *R* values greater than 0.95. There were no *R* values less than 0.847 and the highest *R* value was 1. Fig. 12A shows representative CHs for all three receptor types. Note the responses fall within a 2 ms time frame. The average *R* values for the PC-like population, RA-X group and Merkel-like response was 0.92, 0.99 and 0.9 respectively.

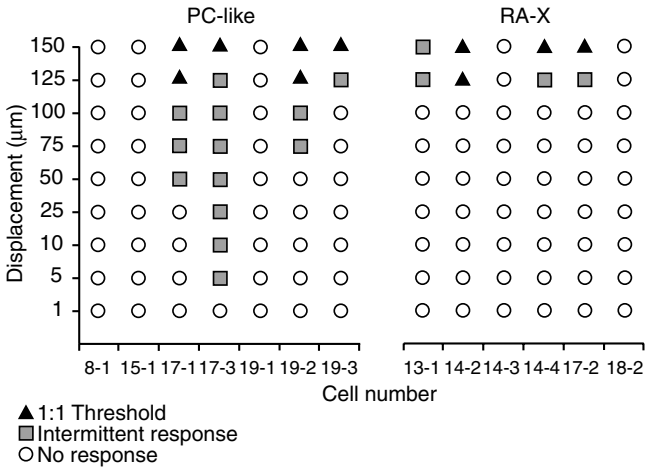

Fig. 8. Graphs of receptor response to multiple static displacement amplitudes for 13 RA receptors divided by subclass. The Pacinian-like (PC-like) group tended to be more sensitive to smaller displacements at absolute levels whereas the rapidly adapting-unknown (RA-X) group was not responsive to displacements smaller than 125 μm.

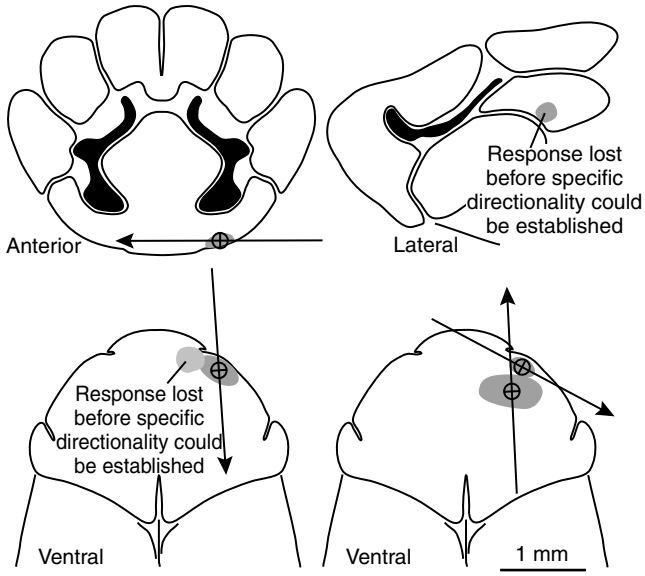

Fig. 9. Receptive fields of directional receptors isolated during the qualitative phase. The arrows indicate the preferred direction. Two cells appeared to be directional but were lost before a specific direction of highest activity could be established.

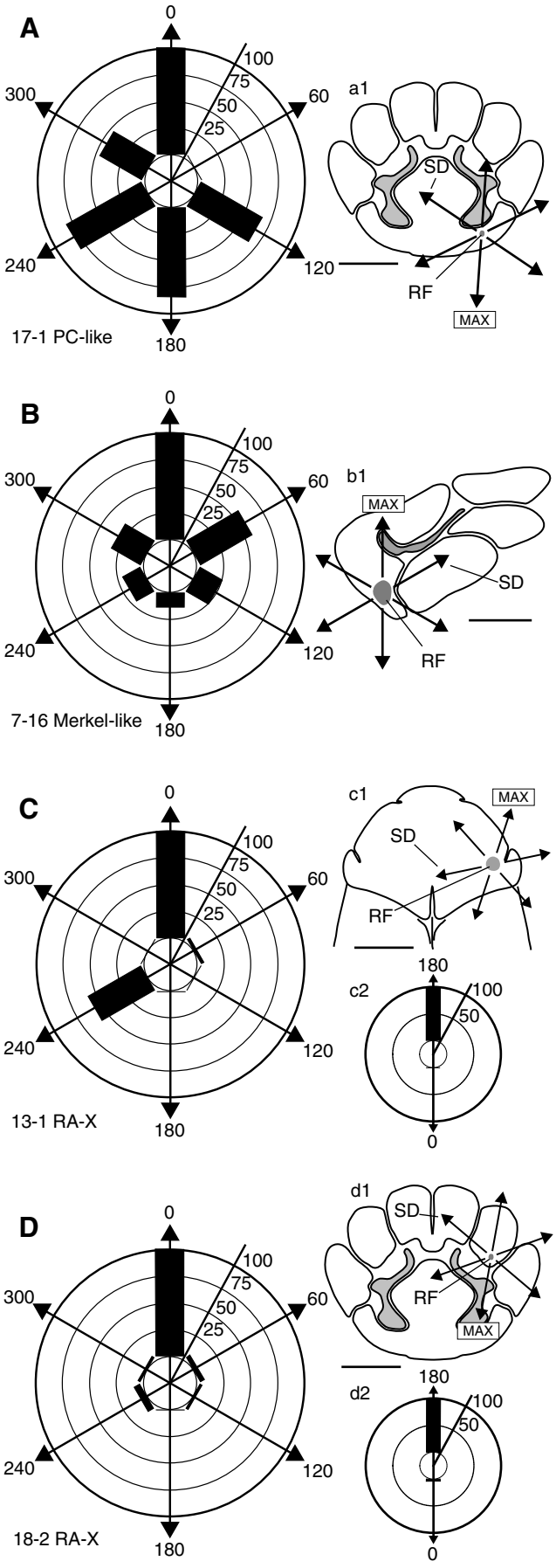

Fig. 10. Representative normalized and rotated circular histograms of directional activity for all three sub-classes of receptor (A–C). The receptive field (RF) and stimulus directions, including the direction of maximum activity (MAX) are depicted to the right (a1–d1). (A) Receptor 17-1 was representative of the Pacinian-like (PC-like) population. This receptor was moderately directionally tuned by the Rayleigh statistic but showed low scores for the tuning ratio (*TR*) and tuning index (*TI*) (see Table 1). (B) Receptor 7-16 was the only slowly adapting response and was strongly directionally tuned. (C) Receptor 13-1 was representative of the rapidly adapting-unknown (RA-X) population. This receptor was strongly directional and responses were inverted when the stimulator was rotated 180° (c2). (D) The most highly directionally tuned receptor found in the study. This receptor scored high on all measures of directionality and responses were inverted when the stimulator was rotated 180° (d2). Scale bars, 1 mm.

Fig. 12B shows the CHs for three receptors with an increased propensity for phase locking. In the least phase locked, the distribution around the mean falls within a 0.8 ms time frame and for the most phase-locked the distribution falls within a 0.4 ms time frame. The variance for each of these CHs is 0.013, 0.012 and 0.007 for cells 14-4, 17-2 and 19-3, respectively. In case 14-4, the temporal coding properties were examined across a range of sinusoidal frequencies (Fig. 12C). In this instance 50 responses were analyzed at each frequency to account for the lower number of responses elicited at non-peak frequencies. This receptor shows the highest degree of temporal fidelity at 10 Hz and it degrades slightly at each increase in frequency. However, even at the least clustered

Table 1. *Summary of values for all measures of directional tuning*

Case no.	Group	Rayleigh *Z* value	Rayleigh *P* value	Tuning ratio	Tuning index
8-1	PC-like	36.09	0.00	0.59	1
15-1	PC-like	7.18	7.63E-04	0.59	3
17-1	PC-like	11.45	1.07E-05	0.63	2
17-3	PC-like	10.55	4.30E-05	0.48	5
18-1	PC-like	0.88	0.41	0.67	0
19-1	PC-like	6.47	0.0020	0.69	2
19-2	PC-like	34.81	0.00	0.56	5
19-3	PC-like	3.32	0.036	0.73	3
13-1	RA-X	46.98	0.00	0.27	5
14-2	RA-X	62.29	0.00	0.61	3
14-3	RA-X	1.81	0.16	0.63	4
14-4	RA-X	20.10	1.86E-09	0.55	5
18-2	RA-X	94.31	0.00	0.19	5
7-16.	Merkel-like	55.46	0.00	0.41	5
8-3	RA-IC	39.48	0.00	0.42	5
9-1	RA-IC	51.08	0.00	0.66	2
14-1	RA-IC	61.01	0.00	0.37	5

PC-like, Pacinian-like; RA-X, rapidly adapting-unknown; RA-IC, rapidly adapting-incomplete classification.

frequency all of the responses fall within a 1 ms time window.

Manipulation of individual Eimer's organs

For three responses, single unit activity was recorded while the receptive field for the neuron was reduced to one, or a few, Eimer's organs under direct stereomicroscopic observation using a handheld probe (Fig. 13). The receptive fields were extremely small. An Eimer's organ is approximately 70 μm or 40 μm in diameter for coast and star-nosed moles, respectively (Catania, 1996; Marasco et al., 2006). In case 19-1 the neuron responded to stimulation of a single Eimer's organ (Fig. 13A). By contrast, the receptive field for neuron 19-4 encompassed four separate, fairly distant organs (Fig. 13B). In the star-nosed mole, the receptive field for one neuron was narrowed down to a single Eimer's organ on the tip of ray 11. Fig. 13C shows the response over 2 s to repeated slight movements of the hand-held probe. For cells 19-1 and 19-4, a blunted insect pin was subsequently mounted on the chubbuck stimulator and responses were collected from each Eimer's organ (Fig. 13A,B right panels).

Discussion

The primary goal of this study was to investigate how Eimer's organs may function to transduce tactile signals. We found that Eimer's organs respond to directional displacements, transducing tactile signals with a high level of spatial and temporal resolution, and some receptors

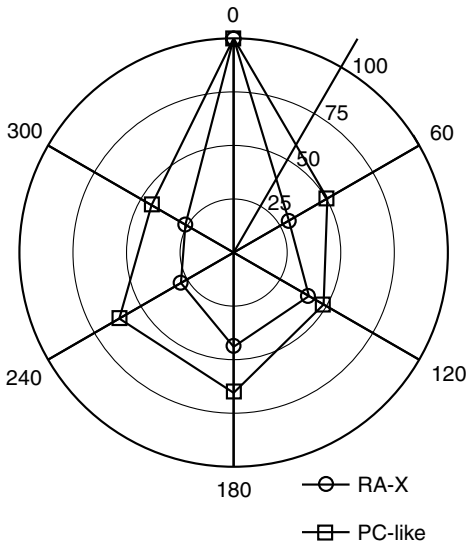

Fig. 11. A graphical comparison of directional tuning between the normalized and rotated average response magnitudes for the Pacinian-like (PC-like) and rapidly adapting-unknown (RA-X) populations. The RA-X population was strongly directionally tuned. The PC-like population was more broadly tuned than the RA-X population.

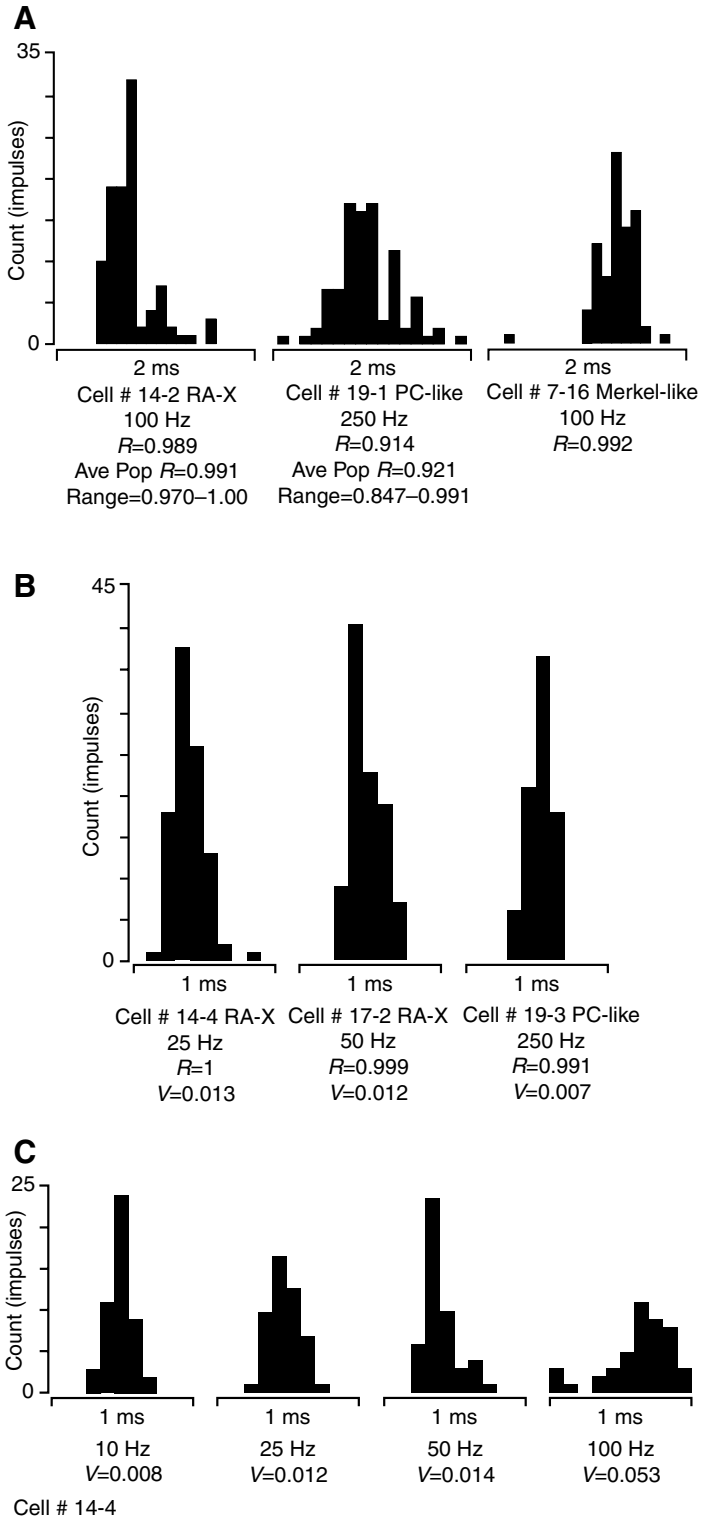

Fig. 12. Cycle histograms relating the precision of temporal patterning to vibrotactile stimuli at peak frequency of activation. (A) Representative cycle histograms from each of the three receptor classes (N=100). (B) Three units with the highest degree of phase locking (N=100). (C) There was adequate data present to calculate cycle histograms across each stimulus frequency for unit number 14-4. As frequency increased the receptor became less phase locked, however, all impulses fell within a 1 ms time frame. V, variance; R, length of mean vector.

have tuning properties that may filter behaviorally irrelevant mechanosensory input. Some responses were consistent with the hypothesis that differential deflection of the ring of nerve terminals in the cell column provides information about surface features on objects that have been touched. Receptive fields were exceptionally small, and this is consistent with the high tactile acuity of moles and the correspondingly high innervation density of the Eimer's organ arrays. These different aspects of Eimer's organ response to mechanosensory stimuli are discussed further below.

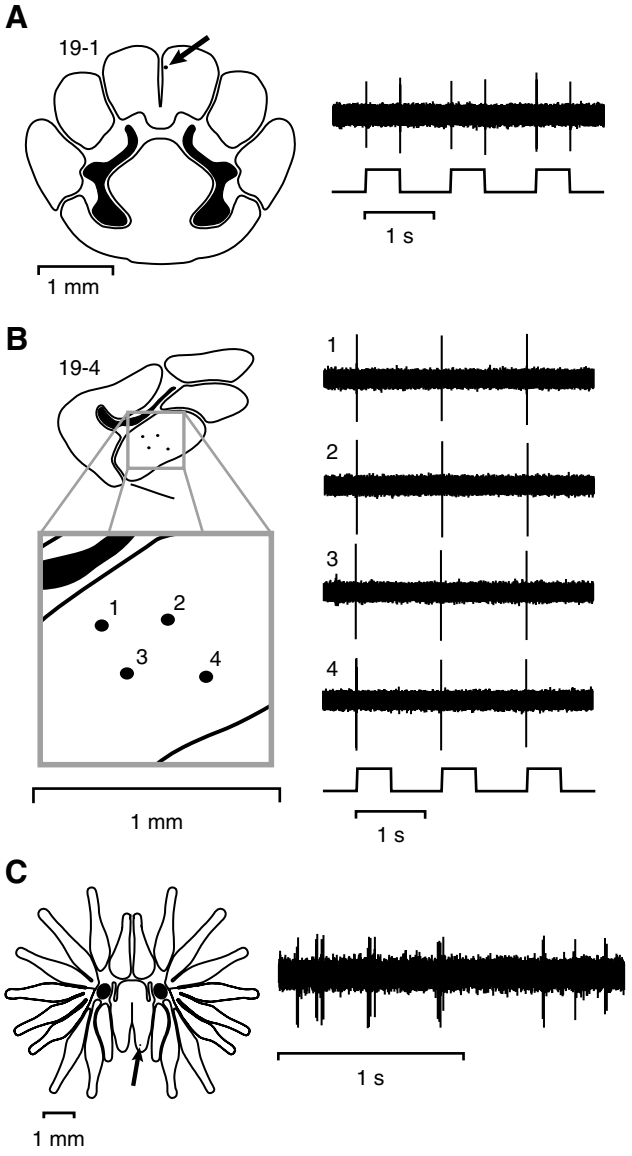

Fig. 13. Receptive field (RF) diagrams for units that were visually attributed to Eimer's organs. (A) RF for an afferent covering a single Eimer's organ in the coast mole. (B) RF for an afferent covering four separate Eimer's organs in the coast mole (1–4). (C) RF for an afferent covering a single Eimer's organ in a star-nosed mole. In A and B the right panels show responses to stimulation of the RF with and insect pin attached to the Chubbuck stimulator. In C responses are shown to a hand-held probe.

Receptive fields

Previous recordings from the neocortex indicate that arrays of Eimer's organs are sensitive to mechanosensory stimuli (Catania and Kaas, 1995; Sachdev and Catania, 2002a; Sachdev and Catania, 2002b) In addition, recent investigation of immunoreactivity of different components of Eimer's organ suggest the three main sensory components of the organ associated with the cell column (Merkel cells, lamellated corpuscles and intraepidermal free nerve endings) are mechanoreceptive (Marasco et al., 2006). In further support of these findings, the results of the present study provide evidence that individual Eimer's organs are responsive to mechanosensory stimulation. This is significant because it is often difficult to isolate individual, small epidermal receptors when recording from afferents (e.g. Iggo et al., 1996) and so the present results regarding small Eimer's organ receptive fields provide new data confirming a mechanosensory function.

The RFs in the coast mole were on average 119 μm across with the smallest RFs for individual Eimer's organs being 70 μm across. In the star-nosed mole the RF for a single receptor was a single 40 μm diameter Eimer's organ. These RFs are much smaller than those reported for glabrous skin in a number of different model systems and probably represent the smallest RFs recorded for a skin surface (Jänig et al., 1968; Talbot et al., 1968; Johansson and Vallbo, 1980; Leem et al., 1993; DiCarlo et al., 1998; Xerri et al., 1998; Vega-Bermudez and Johnson, 1999).

Interestingly, we did not find an obvious difference in the size of RFs of the different receptors classes. This is somewhat surprising, because relative RF size is often used to differentiate between RA receptor classes. For instance, Pacinian responses can be differentiated from other RA responses by their large RFs with indistinct borders (Talbot et al., 1968; Knibestol and Vallbo, 1970) (for a review, see Vallbo and Johansson, 1984). However in Eimer's organ, the lamellated 'Paciniform' corpuscles are much smaller (45 μm) (Marasco et al., 2006) than typical Pacinian receptors (Quilliam and Sato, 1955). In addition, it is possible that the structure of Eimer's organ isolates each receptor complex within the surrounding skin by focusing the tactile input along the cell column (Manger and Pettigrew, 1996) (see also Cauna, 1954). This would also be consistent with the 1:1 ratio of lamellated corpuscles to Eimer's organs – a configuration that would seem redundant if receptive fields were large.

Receptor classes

In the coast mole three main classes of receptor were evident that differed in their response to static indentation. These included one slowly adapting type and two rapidly adapting types. Recordings from the star-nosed mole also suggested this separation into three classes. This division of afferents serving glabrous skin into three classes is well established for a considerable number of different animal model systems and humans (Lindblom, 1965; Jänig et al., 1968; Talbot et al., 1968; Iggo and Ogawa, 1977; Jänig, 1971; Pubols et al., 1971; Pubols and Pubols, Jr, 1973; Johnson, 1974; Dykes and Terzis, 1979;

Johansson and Vallbo, 1979; Ferrington and Rowe, 1980; Vallbo and Johansson, 1984; Gregory et al., 1988; Leem et al., 1993; Iggo et al., 1996; Coleman et al., 2001; Mahns et al., 2003).

Previous histological studies in the mole routinely reveal a preponderance of three main types of receptor end-organ in the glabrous rhinarium (Fig. 1). Eimer's organs are associated with Merkel cell–neurite complexes, Paciniform corpuscles, and intraepidermal free nerve endings (Halata, 1972; Andres and von Düring, 1973; Catania, 1995a; Catania, 1995b; Catania, 1996; Marasco et al., 2006). Based on the average number of receptor subtypes present within each Eimer's organ we would expect 58% of the receptors to be RA and 42% to be SA. The recordings made during the qualitative phase of the experiments revealed a different division of responses: 78.8% RA and 21.2% SA responses. Recordings made during the quantitative phase revealed an even greater bias towards the RA units as 95% of these responses were RA and 4.5% were SA. This difference in actual percentages of the responses probably reflects differential innervation ratios for the different receptors classes, and could also reflect the spatial organization of receptor classes represented within the trigeminal ganglion. Most of the quantitative recording data were obtained from the rostral–medial portion of the exposed ganglion, where the nose representation was most prominent. The larger survey of qualitative receptive fields was obtained from a more evenly distributed sampling of penetrations as there were fewer time constraints during the experiments.

All of the SA responses recorded from the nose in both species of mole compared well to the response profile of typical Merkel cell–neurite complexes (Iggo and Muir, 1969). This electrophysiological characterization is not surprising given the Merkel cell–neurite complexes in Eimer's organ. This is also true for the PC-like responses, as lamellated corpuscles are found at the base of each organ. The characterization of these receptors as PC-like is also suggested by the activity elicited during sinusoidal stimulation between 200 and 300 Hz – another typically Pacinian trait (Sato, 1961). Although the main criterion for distinguishing between the PC-like and RA-X responses was their respective responses to sinusoidal mechanosensory stimulation, there were other differences in response profiles that seemed to distinguish these two receptors. For example the PC-like units tended to be more responsive to lower indentation velocities than the RA-X units (Fig. 7). The PC-like receptors were more sensitive to small amplitude static displacements than the RA-X afferents (Fig. 8). Finally, as a whole, the PC-like units were less directionally sensitive than the RA-X units.

In addition to Merkel cells and lamellated corpuscles, the intraepidermal free nerve endings are the third major sensory component of Eimer's organ evident from anatomical studies. Our finding of three different potential types of mechanoreceptive afferents suggests each major sensory receptor class was represented in our recording data. Interestingly, the responses of RA-X receptors reported here were similar to those reported by Lynn (Lynn, 1969) in the cat. In cats these receptors had very high minimum thresholds for activation and were generally isolated to superficial positions in the epidermis. In addition, they had peak activation through a broad range of lower frequencies and were typically difficult to drive at frequencies greater than 150–200 Hz.

These units were also similar to receptors found by Iggo et al. (Iggo et al., 1996) in the snout skin of the echidna. The push rod sensory end-organ of the monotremes is similar to the Eimer's organ in cellular structure and innervation patterns (Andres and von Düring, 1984; Andres et al., 1991; Manger and Hughes, 1992; Manger and Pettigrew, 1996). Iggo et al. (Iggo et al., 1996) reported RA receptors with high thresholds to stimulation and some that were most responsive to sliding motions of the stimulus probe. These two features parallel the properties of the putative RA-X receptors reported here and may represent analogous receptors in push-rods and Eimer's organs.

Given the preponderance of three major sensory receptors associated with Eimer's organs, and three presumptive response classes from associated afferents, it seemed reasonable to hypothesize which receptors were represented in the recording data. The PC-like and Merkel-like responses presumably correspond to lamellated corpuscles and Merkel cells, respectively. This suggests that the putative RA-X response profile represents the activity of the intraepidermal free nerve endings.

Mole behavior and Eimer's organ stimulation

As the moles forage and move about their tunnels they repeatedly touch the ground with their noses for durations of 30–35 ms. We used high-speed videography to calculate an average velocity of 46.2 mm s^{-1} during nose contact. We subsequently included this velocity in our stimulation paradigm, along with a series of other stimulation velocities. A number of afferents responded to this stimulation velocity in preference to lower velocities (Fig. 7). This was particularly true of the RA-X units.

Two of the units examined occasionally responded with multiple spikes to the ramp stimulus. When the average instantaneous interval frequency for these responses was calculated for each velocity it appeared that these units were coding the velocity of indentation. As the velocity increased the interval frequency increased. Interestingly, both units appeared to be tuned near the behavioral velocity of 46.2 mm s^{-1}. The interval frequency for both increased with increasing velocity up to 46.2 mm s^{-1}. At 84.5 mm s^{-1} the interval frequency for cell 19-4 reached a plateau and the interval frequency for cell 19-2 dropped precipitously. Higher velocities could not be explored because of the mechanical limits of the stimulator.

The results from this stimulation paradigm are consistent with behavioral observations suggesting at least some units are particularly responsive to indentation velocities of

46.2 mm s^{-1}. This could filter some of the tactile stimulation that inevitably occurs when moles are not actively exploring their environments. Further evidence for this possibility comes from the motor component of exploratory behaviors. Both star-nosed moles and Coast moles have a series of tendons that serve to move the modules of Eimer's organs at increased velocities during contact.

Temporal precision

All of the receptors examined from the coast mole nose responded to sinusoidal mechanical stimuli with a high level of temporal precision. When examined collectively the average *R* value for all of the receptors was 0.953 and the least phase locked response corresponded to an *R* value of 0.847. Considering that a receptor with an *R* value greater than 0.3 has a significant capacity for phase locking (Durand and Greenwood, 1958; Bledsoe, Jr et al., 1982; Coleman et al., 2001; Mahns et al., 2003), the fidelity with which the receptors in the mole are able to track a vibratory stimulus is remarkable for the somatosensory system (Mountcastle et al., 1969; Greenstein et al., 1987; Vickery et al., 1992; Coleman et al., 2001; Mahns et al., 2003). The temporal acuity of responses, as measured by the time span of the entire distribution of impulses around the mean for the three most phase locked cells, was within an order of magnitude of similar distributions reported for primary afferents in electric fish (*Eigenmannia*) and magnocellular neurons in barn owls (Sullivan and Konishi, 1984; Rose and Heiligenberg, 1985; Carr et al., 1986; Carr and Konishi, 1990).

Directional sensitivity and the function of Eimer's organ

The conspicuous circular organization of nerve endings (Fig. 1) and its innervation pattern in Eimer's organs (Marasco et al., 2006) and push-rods (Andres and von Düring, 1984) has led to speculation that both organs may transduce directional information (Quilliam, 1966a; Andres and von Düring, 1984; Catania, 1996; Catania, 2000; Marasco et al., 2006). In support of this possibility, we noticed that some responses in the present study were elicited by stimuli applied in a specific direction when using a hand-held probe (Fig. 9). These receptors could be brushed in one direction to elicit a strong response but when brushed in other directions were silent. To provide more consistent and controlled directional stimulation, a piezo-electric sweeping stimulator was used to provide directional displacements.

The recordings resulting from these trials revealed that nearly all of the receptors examined had a preference for particular directions of applied stimuli with respect to multiple measures of directionality (Table 1). Two cells in particular, 13-1 and 18-2, were almost exclusively unidirectional (Fig. 10C,D). These two units were also classified as RA-X receptors, and possibly represent the free nerve endings in the cell column. In all, most of the RA-X units were well tuned to directional input. The Merkel cell–neurite complex also showed a strong directional response suggesting the structure of the Eimer's organ allows for transduction of directional displacements to the deep layers of the epidermis (Manger and Pettigrew, 1996) (see also Cauna, 1954). In general, the PC-like units were also directionally tuned, however, this group was less robustly directional than the RA-X group (Fig. 11).

Together these data support the hypothesis that one of the functions of Eimer's organ is to transduce directional displacements of the central cell column. However, it is important to point out that our directional stimulation paradigm does not mimic natural stimuli. Moles make single brief contacts to the substrate or objects while searching their environment, and do not slide or rub the nose over objects. In a behaving mole, the direction stimulation of the cell column that we propose would probably result from the mechanical deflections caused by small surface features as the Eimer's organs are compressed against an object (Fig. 14A–C). Presumably such direction displacements would reveal patterns representing fine surface details and contours.

If this is indeed a basic component of Eimer's organ function, a simple and powerful model for coding shapes and textures naturally follows when one considers the integration of information from a skin surface containing multiple Eimer's organs. Fig. 14 outlines this proposal in schematic form. The main feature of this proposal is the differential stimulation of terminal neurites in the cell column indicating the direction of deflection for each Eimer's organ. Information from a single Eimer's organ would be of little use, but the deflection of groups of Eimer's organs in unison, or in opposition, could reliably indicate the shape and relative location of curves and edges of objects. This is illustrated for a sphere and a cylinder applied to an array of Eimer's organs in Fig. 14H,I. Note that a single compression of the skin surface against the objects is sufficient for generating the stereotypic output signaling the different shapes. This would explain a hallmark feature of mole tactile behavior – that single short, but firm touches to objects are the unit of mechanosensory behavior in these species. Invertebrate prey items exhibit ample textural cues in the appropriate size range, such as repeated ridges, spines, and cuticular segments, which would allow moles to distinguish prey items by this mechanism.

List of abbreviations

CH	cycle histogram
DS	directionally sensitive
PC-like	Pacinian-like
R	length of the mean vector
RA	rapidly adapting
RA-IC	RA-incomplete
RA-X	RA-unknown
RF	receptive field
Rz	Rayleigh Z value
SA	slowly adapting
TI	tuning index
TR	tuning ratio

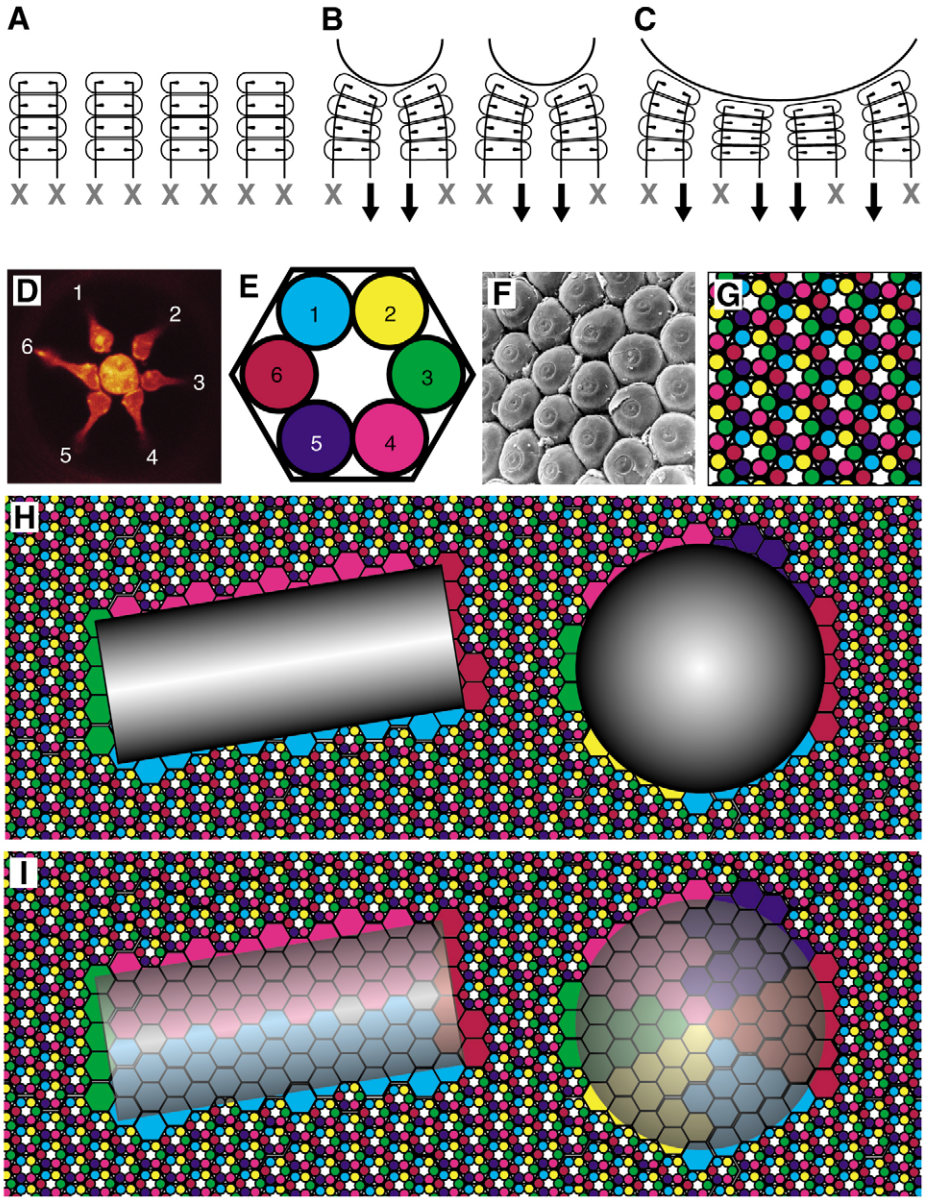

Fig. 14. The hypothetical function of Eimer's organ. Each organ is depicted schematically as a stack of epithelial cells with the free nerve endings running up each side. This structural configuration may allow for a tactile 'snapshot' each time the nose touches a surface. Maximally active free nerve endings are indicated with an arrow. (A) The Eimer's organs with no tactile stimulus. (B) Hypothetical response to small, spherical surface features. (C) Hypothetical response to larger contours. (D) The free nerve terminals at the surface of an Eimer's organ in the star-nosed mole revealed with DiI. Each satellite terminal is given a number to represent position. (E) Schematic representation of the numbered terminals color-coded and arranged in a hexagon. (F) A scanning electron micrograph of the surface of the nose of the star-nosed mole showing Eimer's organs in a hexagonal array. (G) Schematized Eimer's organs with color-coded nerve terminals in a hexagonal array. (H) Eimer's organs compressed by a cylinder and a sphere. The color of the deflected hexagon reflects the direction of maximal displacement. (I) The two objects have been made translucent. The deflected Eimer's organs generate a stereotypic output signaling the shape and contours of the applied stimulus.

We thank Terry Page for help with all facets of the analysis of the electrophysiology data. Corrie Camalier and Jamie Reed for editorial suggestions. We also thank Mary Dietrich of the Vanderbilt University Advanced Computing Center for Research and Education for help with the statistical analysis. Thanks to Kevin Campbell and Tim Sheehan for supplying Coast moles. Special thanks go to the Vanderbilt Department of Animal Care for husbandry of moles. This work was sponsored by National Science Foundation (grant numbers: 0238364 and 0518819).

References

Allison, T. and Van Twyver, H. (1970). Sensory representation in the neocortex of the mole, *Scalopus aquaticus*. *Exp. Neurol.* **27**, 554-563.

Andres, K. H. and von Düring, M. (1973). Morphology of cutaneous receptors. In *Handbook of Sensory Physiology, Vol. 2, Somatosensory System* (ed. A. Iggo), pp. 3-28. Berlin: Springer-Verlag.

Andres, K. H. and von Düring, M. (1984). The platypus bill. A structural and functional model of a pattern-like arrangement of different cutaneous sensory receptors. In *Sensory Receptor Mechanisms* (ed. W. Hamann and A. Iggo), pp. 81-89. Singapore: World Scientific Publishing Company.

Andres, K. H., von Düring, M., Iggo, A. and Proske, U. (1991). The anatomy and fine structure of the echidna *Tachyglossus aculeatus* snout with respect to its different trigeminal sensory receptors including the electroreceptors. *Anat. Embryol.* **184**, 371-393.

Batschelet, E. (1981). *Circular Statistics in Biology*. New York: Academic Press.

Bielschowsky, M. (1907). Ueber sensible Nervenendigungen in der Haut zweier Insectivoren (*Talpa europaea* und *Centetes ecaudatus*). *Anat. Anz.* **31**, 187-194.

Bledsoe, S. C., Jr, Rupert, A. L. and Moushegian, G. (1982). Response characteristics of cochlear nucleus neurons to 500-Hz tones and noise: findings relating to frequency-following potentials. *J. Neurophysiol.* **47**, 113-127.

Boeke, J. (1932). Nerve endings, motor and sensory. In *Cytology and Cellular Pathology of the Nervous System* (ed. W. Penfield), pp. 243-309. New York: Paul B. Hoeber.

Boeke, J. (1940). *Problems of Nervous Anatomy*. London: Oxford University Press.

Boeke, J. and de Groot, G. J. (1907). Physiologische regenerate van neurofibrillaire eindretten. *Versl. Gewone Vergad. Afd. Natuurkd. K. Ned. Akad. Wet.* **16**, 319-325.

Bolanowski, S. J., Jr and Zwislocki, J. J. (1984). Intensity and frequency characteristics of Pacinian corpuscles. I. Action potentials. *J. Neurophysiol.* **51**, 793-811.

Botezat, E. (1903). Ueber die epidermoidalen Tastapparate in der Schnauze des Maulwurfs und anderer Säugetiere mit besonderer Berücksichtigung derselben für die Phylogenie der Haare. *Arch. Mikr. Anat.* **61**, 730-764.

Carr, C. E. and Konishi, M. (1990). A circuit for detection of interaural time differences in the brain stem of the barn owl. *J. Neurosci.* **10**, 3227-3246.

Carr, C. E., Heiligenberg, W. and Rose, G. J. (1986). A time-comparison circuit in the electric fish midbrain. I. Behavior and physiology. *J. Neurosci.* **6**, 107-119.

Catania, K. C. (1995a). Structure and innervation of the sensory organs on the snout of the star-nosed mole. *J. Comp. Neurol.* **351**, 536-548.

Catania, K. C. (1995b). A comparison of the Eimer's organs of three North American moles: the hairy-tailed mole (*Parascalops breweri*), the star-nosed mole (*Condylura cristata*), and the eastern mole (*Scalopus aquaticus*). *J. Comp. Neurol.* **354**, 150-160.

Catania, K. C. (1996). Ultrastructure of the Eimer's organ of the star-nosed mole. *J. Comp. Neurol.* **365**, 343-354.

Catania, K. C. (2000). Epidermal sensory organs of moles, shrew moles, and desmans: a study of the family Talpidae with comments on the function and evolution of Eimer's organ. *Brain Behav. Evol.* **56**, 146-174.

Catania, K. C. and Kaas, J. H. (1995). Organization of the somatosensory cortex of the star-nosed mole. *J. Comp. Neurol.* **351**, 549-567.

Catania, K. C. and Kaas, J. H. (1997). Somatosensory fovea in the star-nosed mole: behavioral use of the star in relation to innervation patterns and cortical representation. *J. Comp. Neurol.* **387**, 215-233.

Catania, K. C. and Remple, F. E. (2004). Tactile foveation in the star-nosed mole. *Brain Behav. Evol.* **63**, 1-12.

Catania, K. C. and Remple, F. E. (2005). Asymptotic prey profitability drives star-nosed moles to the foraging speed limit. *Nature* **433**, 519-522.

Catania, K. C., Lyon, D. C., Mock, O. B. and Kaas, J. H. (1999). Cortical organization in shrews: evidence from five species. *J. Comp. Neurol.* **410**, 55-72.

Cauna, N. (1954). Nature and functions of the papillary ridges of the digital skin. *Anat. Rec.* **119**, 449-468.

Cauna, N. and Alberti, P. (1961). Nerve supply and distribution of cholinesterase activity in the external nose of the mole. *Z. Zellforsch. Mikrosk. Anat.* **54**, 158-166.

Chubbuck, J. G. (1966). Small motion biological stimulator. *APL Tech. Digest* **5**, 18-23.

Coleman, G. T., Bahramali, H., Zhang, H. Q. and Rowe, M. J. (2001). Characterization of tactile afferent fibers in the hand of the marmoset monkey. *J. Neurophysiol.* **85**, 1793-1804.

DiCarlo, J. J., Johnson, K. O. and Hsiao, S. S. (1998). Structure of receptive fields in area 3b of primary somatosensory cortex in the alert monkey. *J. Neurosci.* **18**, 2626-2645.

Dogiel, A. S. (1903). Über die Nervenendapparate in der Haut des Menschen. *Z. Wiss. Zool.* **65**, 46.

Durand, D. and Greenwood, J. A. (1958). Modifications of the Rayleigh test for uniformity in analysis of two-dimensional orientation data. *J. Geol.* **66**, 229-238.

Dykes, R. W. and Terzis, J. K. (1979). Reinnervation of glabrous skin in baboons: properties of cutaneous mechanoreceptors subsequent to nerve crush. *J. Neurophysiol.* **42**, 1461-1478.

Eimer, T. (1871). Die Schnautze des Maulwurfs als Tastwerkzeug. *Arch. Mikr. Anat.* **7**, 181-191.

Ferrington, D. G. and Rowe, M. J. (1980). Functional capacities of tactile afferent fibres in neonatal kittens. *J. Physiol.* **307**, 335-353.

Fisher, N. I. (1993). *Statistical Analysis of Circular Data*. Cambridge: Cambridge University Press.

Gibson, J. M. and Welker, W. I. (1983). Quantitative studies of stimulus coding in first-order vibrissa afferents of rats. 2. Adaptation and coding of stimulus parameters. *Somatosens. Res.* **1**, 95-117.

Gorman, M. L. and Stone, R. D. (1990). *The Natural History of Moles*. Ithaca, NY: Cornell University Press.

Greenstein, J., Kavanagh, P. and Rowe, M. J. (1987). Phase coherence in vibration-induced responses of tactile fibres associated with Pacinian corpuscle receptors in the cat. *J. Physiol.* **386**, 263-275.

Gregg, J. M. and Dixon, A. D. (1973). Somatotopic organization of the trigeminal ganglion in the rat. *Arch. Oral Biol.* **18**, 487-498.

Gregory, J. E., Iggo, A., McIntyre, A. K. and Proske, U. (1988). Receptors in the bill of the platypus. *J. Physiol.* **400**, 349-366.

Groeneweg, W. (1923). Over de Ontwikkeling van het orgaan van Eimer in den Snuit van den mol. PhD Thesis, University of Utrecht, Utrecht, The Netherlands.

Halata, Z. (1972). Innervation der unbehaarten Nasenhaut des Maulwurfs (*Talpa europaea*) I. Intraepidermale Nervenendigungen. *Z. Zellforsch. Mikrosk. Anat.* **125**, 108-120.

Iggo, A. and Muir, A. R. (1969). The structure and function of a slowly adapting touch corpuscle in hairy skin. *J. Physiol.* **200**, 763-796.

Iggo, A. and Ogawa, H. (1977). Correlative physiological and morphological studies of rapidly adapting mechanoreceptors in cat's glabrous skin. *J. Physiol.* **266**, 275-296.

Iggo, A., Gregory, J. E. and Proske, U. (1996). Studies of mechanoreceptors in skin of the snout of the echidna *Tachyglossus aculeatus*. *Somatosens. Mot. Res.* **13**, 129-138.

Jänig, W. (1971). Morphology of rapidly and slowly adapting mechanoreceptors in the hairless skin of the cat's hind foot. *Brain Res.* **28**, 217-231.

Jänig, W., Schmidt, R. F. and Zimmermann, M. (1968). Single unit responses and the total afferent outflow from the cat's foot pad upon mechanical stimulation. *Exp. Brain Res.* **6**, 100-115.

Johansson, R. S. and Vallbo, A. B. (1979). Tactile sensibility in the human hand: relative and absolute densities of four types of mechanoreceptive units in glabrous skin. *J. Physiol.* **286**, 283-300.

Johansson, R. S. and Vallbo, A. B. (1980). Spatial properties of the population of mechanoreceptive units in the glabrous skin of the human hand. *Brain Res.* **184**, 353-366.

Johansson, R. S., Landstrom, U. and Lundstrom, R. (1982). Responses of mechanoreceptive afferent units in the glabrous skin of the human hand to sinusoidal skin displacements. *Brain Res.* **244**, 17-25.

Johnson, K. O. (1974). Reconstruction of population response to a vibratory stimulus in quickly adapting mechanoreceptive afferent fiber population innervating glabrous skin of the monkey. *J. Neurophysiol.* **37**, 48-72.

Kadanoff, D. (1928). Über die intraepithelialen Nerven und ihre Endigungen beim Menschen und bei den Säugetieren. *Z. Zellforsch. Mikr. Anat.* **7**, 553-576.

Knibestol, M. and Vallbo, A. B. (1970). Single unit analysis of mechanoreceptor activity from the human glabrous skin. *Acta Physiol. Scand.* **80**, 178-195.

Lavine, R. A. (1971). Phase-locking in response of single neurons in cochlear nuclear complex of the cat to low-frequency tonal stimuli. *J. Neurophysiol.* **34**, 467-483.

Leem, J. W., Willis, W. D. and Chung, J. M. (1993). Cutaneous sensory receptors in the rat foot. *J. Neurophysiol.* **69**, 1684-1699.

Lindblom, U. (1965). Properties of touch receptors in distal glabrous skin of the monkey. *J. Neurophysiol.* **28**, 966-985.

Loewenstein, W. R. (1958). Generator processes of repetitive activity in a pacinian corpuscle. *J. Gen. Physiol.* **41**, 825-845.

Lynn, B. (1969). The nature and location of certain phasic mechanoreceptors in the cat's foot. *J. Physiol.* **201**, 765-773.

Mahns, D. A., Coleman, G. T., Ashwell, K. W. S. and Rowe, M. J. (2003). Tactile sensory function in the forearm of the monotreme *Tachyglossus aculeatus*. *J. Comp. Neurol.* **459**, 173-185.

Manger, P. R. and Hughes, R. L. (1992). Ultrastructure and distribution of epidermal sensory receptors in the beak of the echidna, *Tachyglossus aculeatus*. *Brain Behav. Evol.* **40**, 287-296.

Manger, P. R. and Pettigrew, J. D. (1996). Ultrastructure, number, distribution and innervation of electroreceptors and mechanoreceptors in the bill skin of the platypus, *Ornithorhynchus anatinus*. *Brain Behav. Evol.* **48**, 27-54.

Marasco, P. D., Tsuruda, P. R., Bautista, D. M., Julius, D. and Catania, K. C. (2006). Neuroanatomical evidence for segregation of nerve fibers conveying light touch and pain sensation in Eimer's organ of the mole. *Proc. Natl. Acad. Sci. USA* **103**, 9339-9344.

Merkel, F. (1875). Tastzellen und Tastkörperchen bei den Hausthieren und beim Menschen. *Arch. Mikr. Anat.* **11**, 636-652.

Merkel, F. (1880). *Über die Endigungen der sensiblen Nerven in der Haut der Wirbelthiere*. Rostock: H. Schmidt.

Minnery, B. S. and Simons, D. J. (2003). Response properties of whisker-associated trigeminothalamic neurons in rat nucleus principalis. *J. Neurophysiol.* **89**, 40-56.

Mountcastle, V. B., Talbot, W. H., Sakata, H. and Hyvarinen, J. (1969).

Cortical neuronal mechanisms in flutter-vibration studied in unanesthetized monkeys. Neuronal periodicity and frequency discrimination. *J. Neurophysiol.* **32**, 452-484.

Pubols, L. M. and Pubols, B. H., Jr (1973). Modality composition and functional characteristics of dorsal column mechanoreceptive afferent fibers innervating the raccoon's forepaw. *J. Neurophysiol.* **36**, 1023-1037.

Pubols, L. M., Pubols, B. H., Jr and Munger, B. L. (1971). Functional properties of mechanoreceptors in glabrous skin of the raccoon's forepaw. *Exp. Neurol.* **31**, 165-182.

Quilliam, T. A. (1966a). The mole's sensory apparatus. *J. Zool.* **149**, 76-88.

Quilliam, T. A. (1966b). Structure of receptor organs: unit design and array patterns in receptor organs. In *Touch, Heat and Pain* (ed. A. V. S. De Reuck and J. Knight), pp. 86-116. Boston: Little, Brown and Company.

Quilliam, T. A. and Sato, M. (1955). The distribution of myelin on nerve fibres from Pacinian corpuscles. *J. Physiol.* **129**, 167-176.

Ranvier, L. (1880). On the terminations of nerves in the epidermis. *Q. J. Microsc. Sci.* **20**, 456-458.

Ranvier, L. (1889). *Traité technique d'Histologie* (2nd edn). Paris: F. Savy.

Retzius, G. (1892). Ueber die sensiblen Nervenendigungen in den Epithelien bei den Wirbelthieren. *Biol. Untersuch.* **4**, 37-44.

Rose, G. and Heiligenberg, W. (1985). Temporal hyperacuity in the electric sense of fish. *Nature* **318**, 178-180.

Sachdev, R. N. and Catania, K. C. (2002a). Effects of stimulus duration on neuronal response properties in the somatosensory cortex of the star-nosed mole. *Somatosens. Mot. Res.* **19**, 272-278.

Sachdev, R. N. and Catania, K. C. (2002b). Receptive fields and response properties of neurons in the star-nosed mole's somatosensory fovea. *J. Neurophysiol.* **87**, 2602-2611.

Sato, M. (1961). Response of Pacinian corpuscles to sinusoidal vibration. *J. Physiol.* **159**, 391-409.

Sullivan, W. E. and Konishi, M. (1984). Segregation of stimulus phase and intensity coding in the cochlear nucleus of the barn owl. *J. Neurosci.* **4**, 1787-1799.

Talbot, W. H., Darian-Smith, I., Kornhuber, H. H. and Mountcastle, V. B. (1968). The sense of flutter-vibration: comparison of the human capacity with response patterns of mechanoreceptive afferents from the monkey hand. *J. Neurophysiol.* **31**, 301-334.

Vallbo, A. B. and Johansson, R. S. (1984). Properties of cutaneous mechanoreceptors in the human hand related to touch sensation. *Hum. Neurobiol.* **3**, 3-14.

Vega-Bermudez, F. and Johnson, K. O. (1999). SA1 and RA receptive fields, response variability, and population responses mapped with a probe array. *J. Neurophysiol.* **81**, 2701-2710.

Vickery, R. M., Gynther, B. D. and Rowe, M. J. (1992). Vibrotactile sensitivity of slowly adapting type I sensory fibres associated with touch domes in cat hairy skin. *J. Physiol.* **453**, 609-626.

Xerri, C., Merzenich, M. M., Peterson, B. E. and Jenkins, W. (1998). Plasticity of primary somatosensory cortex paralleling sensorimotor skill recovery from stroke in adult monkeys. *J. Neurophysiol.* **79**, 2119-2148.

Zar, J. H. (1999). *Biostatistical Analysis* (4th edn). Upper Saddle River, NJ: Prentice Hall.